Valine 10 May Act as a Driver for Product Release from the Active Site of Human Glutathione Transferase P1-1[†,‡]

Chiara Micaloni,[§] Anna P. Mazzetti,[§] Marzia Nuccetelli,[§] Jamie Rossjohn,[∥] William J. McKinstry,[∥] Giovanni Antonini,[⊥,#] Anna M. Caccuri,[§] Aaron J. Oakley,[∥,○] Giorgio Federici,[▽] Giorgio Ricci,[§] Michael W. Parker,[∥] and Mario Lo Bello*[,§]

Department of Biology, University of Rome "Tor Vergata", Via della Ricerca Scientifica, 00133 Roma, Italy, The Ian Potter Foundation Protein Crystallography Laboratory, St. Vincent's Institute of Medical Research, Fitzroy, Victoria 3065, Australia, Department of Pure and Applied Biology, University of L'Aquila, Coppito, 67010 L'Aquila, Italy, Department of Biochemical Sciences "Alessandro Rossi Fanelli", University of Rome "La Sapienza", Piazzale Aldo Moro 5, 00185 Roma, Italy, and Children's Hospital IRCCS "Bambino Gesù", Piazza S. Onofrio 4, 00165 Roma, Italy

Received March 29, 2000; Revised Manuscript Received September 22, 2000

ABSTRACT: We have probed the electrophilic binding site (H-site) of human glutathione transferase P1-1 through mutagenesis of two valines, Val 10 and Val 35, into glycine and alanine, respectively. These two residues were previously shown to be the only conformationally variable residues in the H-site and hence may play important roles in cosubstrate recognition and/or product dissociation. Both of these mutant enzymes have been expressed in *Escherichia coli* and purified and their kinetic properties characterized. The results demonstrate that Val35Ala behaves similarly to wild-type, whereas Val10Gly exhibits a strong decrease of k_{cat} and k_{cat}/K_m ^{cosub} toward two selected cosubstrates: ethacrynic acid and 1-chloro-2,4-dinitrobenzene. Pre-steady-state kinetic analysis of the GSH conjugation with ethacrynic acid shows that both wild-type and Val10Gly mutant enzymes exhibit the same rate-limiting step: the dissociation of product. However, in the Val10Gly mutant there is an increased energetic barrier which renders the dissociation of product more difficult. Similar results are found for the Val10Gly mutant with 1-chloro-2,4-dinitrobenzene as cosubstrate. With this latter cosubstrate, Val 10 also exerts a positive role in the conformational transitions of the ternary complex before the chemical event. Crystallographic analysis of the Val10Gly mutant in complex with the inhibitor *S*-hexyl-GSH suggests that Val 10 optimally orientates products, thus promoting their exit from the active site.

Glutathione transferases (EC 2.5.1.18) (GSTs)[1] are a family of enzymes involved in cellular detoxification by catalyzing the nucleophilic attack of GSH on the electrophilic center of a number of toxic compounds and xenobiotics (*1*). These cytosolic enzymes have been grouped into at least nine species-independent classes (Alpha, Beta, Delta, Kappa, Mu, Pi, Sigma, Theta and Zeta) on the basis of their amino acid sequence, substrate specificity, and immunological properties (*2*−*8*). For a more detailed review on the molecular properties of GSTs, see ref *9*.

Human placental glutathione transferase (class Pi) (GST P1-1) (*10*), a homodimeric protein of about 46 kDa, has been extensively studied in different laboratories because of its potential use as a marker during chemical carcinogenesis (*11*, *12*) and its possible role in the mechanism of cellular multidrug resistance against a number of anti-neoplastic agents (*13*−*15*). Recent advances suggest a role for GST P1-1 in the regulation of Jun kinase protein (a stress-activated protein which phosphorylates c-Jun) (*16*) and as a "tissue" transglutaminase-specific substrate in neural cells committed to apoptosis (*17*). Crystallographic and site-directed mutagenesis studies have indicated that a number of residues are involved in GSH recognition and binding (*18*−*22*). The high-resolution structures of human GST P1-1, complexed with GSH analogues or inhibitors (*20*, *22*−*26*), also help to define the xenobiotic substrate binding site (H-site). The H-site walls are lined by residues Phe 8, Val 35, Ile 104, and Tyr 108, and the base is formed by Val 10 and Gly 205. Although these residues are hydrophobic, the H-site is

[†] This work was supported in part by an Australian Research Council Project Grant and an Australian Research Council Senior Research Fellowship (to M.W.P.), a National Research Council of Italy Grant (Target Project on Biotechnology) (to G.A. and G.R.), a 40% MURST (to G.R.), a National Health & Medical Research Council Postgraduate Research Scholarship and an International Centre for Diffraction Data Crystallography Scholarship (to A.J.O.), and an Australian Research Council Postdoctoral Fellowship (to J.R.).

[‡] The crystallographic coordinates have been deposited in the Brookhaven Protein Data Bank under the filename 23GS.

* Address correspondence to this author. Fax: 39 06 2023500. E-mail: Lobello@uniroma2.it.

[§] University of Rome "Tor Vergata".

[∥] St. Vincent's Institute of Medical Research.

[⊥] University of L'Aquila.

[#] University of Rome "La Sapienza".

[○] Present address: Department of Pharmacology, The Queen Elizabeth II Medical Centre, Nedlands, Western Australia 6009, Australia.

[▽] Children's Hospital IRCCS "Bambino Gesù".

[1] Abbreviations: CDNB, 1-chloro-2,4-dinitrobenzene; FDNB, 1-fluoro-2,4-dinitrobenzene; DNP-GSH, 2,4-dinitrophenylglutathione; DTT, 1,4-dithiothreitol; EA, ethacrynic acid; GS−EA, glutathione conjugate of ethacrynic acid; EDTA, ethylenediaminetetraacetic acid; GSH, glutathione; GST, glutathione transferase; LB, Luria broth; MES, 2-(*N*-morpholino)ethanesulfonic acid; NBC, *p*-nitrobenzyl chloride; NBD-Cl, 7-chloro-4-nitrobenzo-2-oxa-1,3-diazole; 4-NQO, 4-nitroquinoline 1-oxide; SDS−PAGE, sodium dodecyl sulfate−polyacrylamide gel electrophoresis; WT, wild-type enzyme.

10.1021/bi0007122 CCC: $19.00
Published on Web 12/02/2000

quite open and subdivided into two distinct portions: one more hydrophobic, formed by a cluster of Tyr 7, Phe 8, and Val 10 residues, and one more hydrophilic, contributed by Ile 104, Tyr 108, Asn 204, and Gly 205 residues (*23*, *25*). In fact, this latter portion is filled with a network of water molecules that may interact with polar substrates or polar moieties of hydrophobic substrate bound to the H-site. Thus on the basis of all these structural data, the H-site is now well defined. However, to understand the substrate selectivity of the enzyme, it is necessary to elucidate the role of each of the above residues by site-directed mutagenesis. For example, Tyr 7 has been extensively studied in different GST classes where it appears to stabilize the thiolate ion of the bound GSH (*9*). Tyr 108 (with its hydroxyl group) possesses a catalytic role in the GSH/ethacrynic acid conjugation reaction and influences both catalysis and affinity of the cosubstrate in the GSH−7-chloro-4-nitrobenz-2-oxa-1,3-diazole conjugation (*27*). Ile 104 plays multiple roles including a contribution to the geometry of the H-site due its hydrophobic side chain, influencing the enzymatic activity by interacting with Tyr 108 and affecting the thermal stability of GST P1-1 (*28*, *29*). The aim of the present work is to study the role of the valine residues contributing to the H-site: Val 10 and Val 35. These two residues were previously shown to be the only conformationally variable residues in the H-site: Val 10 can adopt different rotameric states and Val 35 can be highly mobile (*23*). Hence these residues may play important roles in cosubstrate recognition and/or product dissociation. Both these residues have been mutated, by site-directed mutagenesis, into Gly and Ala, respectively, expressed in *Escherichia coli*, and purified and their enzymatic properties characterized toward a range of hydrophobic substrates. These mutants were designed to reduce the size of the hydrophobic side chain. In the case of Val 10 we mutated this residue into Gly to see the effect of the complete removal of any side chain which could interact (via van der Waals contacts) with the hydrophobic cosubstrate. The results show that the Val 10 mutation to Gly markedly affects k_{cat} toward the cosubstrates, 1-chloro-2,4-dinitrobenzene (CDNB) and ethacrynic acid (EA), while the Val35Ala mutant appears to behave very similarly to the WT enzyme. The role of Val 10 has been further evaluated by crystallographic, kinetic, and spectroscopic approaches. It is proposed that this residue, located at the base of the H-site, may help to orient products optimally before their exit from the active site.

EXPERIMENTAL PROCEDURES

Expression Plasmids and Site-Directed Mutagenesis. The plasmid pGST-1, producing large amounts of recombinant WT GST P1-1 in the cytoplasm of *E. coli*, has previously been described (*30*). The expression plasmids pGST-4 and p18Seq-1, previously described (*27*, *31*), were used to generate the single-stranded DNA template used for site-directed mutagenesis according to the method described by Kunkel and co-workers with minor modifications (*31*, *32*). The following oligonucleotides—Gly 10, 5′-CGGCCTC-GAGCCGGGAAGT, and Ala 35, 5′-CACGTCTCCGCG-GTCACGT—were used as mutagenic primers for the Val10Gly and Val35Ala mutations, respectively. The nucleotide sequences of the plasmids carrying the Val10Gly (pGST-G10) and Val35Ala (pGST-A35) mutations were verified by the dideoxy chain termination method.

Protein Expression and Purification. WT and mutant GST P1-1 enzymes were produced as previously described (*30*, *31*). Briefly, TOP 10 *E. coli* cells, harboring plasmid pGST-1 or plasmids pGST-G10 and pGST-A35, were grown in LB medium containing 100 μg/mL ampicillin and 50 μg/mL streptomycin. The synthesis of GST was induced by the addition of 0.2 mM isopropyl 1-thio-β-galactopyranoside when the absorbance at 600 nm was 0.5. Eighteen hours after induction, cells were harvested by centrifugation and lysed as previously described (*30*). WT and GST mutant enzymes were purified by affinity chromatography on immobilized glutathione (*33*). After affinity purification, the WT and the mutant enzymes (Val10Gly and Val35Ala) were homogeneous as judged by SDS−PAGE (*34*). The protein concentration was determined by the method of Lowry et al. (*35*).

Kinetic Studies. The enzymatic activities were determined spectrophotometrically at 25 °C with different cosubstrates under the conditions reported below. Spectrophotometric measurements were performed in a double beam Uvicon 940 spectrophotometer (Kontron Instruments) equipped with a thermostated cuvette compartment. Initial rates were measured at 0.1 s intervals for a total period of 12 s after a lag time of 5 s. Enzymatic rates were corrected for the spontaneous reaction.

Apparent kinetic parameters, k_{cat}, K_m^{cosub}, and k_{cat}/K_m^{cosub} (reported in Table 1), for different cosubstrates were determined at fixed concentrations of GSH and variable concentrations of electrophilic substrate, by fitting the collected data to the Michaelis−Menten equation by nonlinear regression analysis using the Graph PAD Prism (Graph PAD Software, San Diego, CA). Experimental conditions for each substrate were as follows: (1) 0.025−0.4 mM EA in the presence of 0.25 mM GSH in 0.1 M potassium phosphate buffer, pH 6.5. Apparent K_m^{GSH} was obtained at fixed EA concentration (0.4 mM) and variable GSH concentration (from 0.025 to 0.5 mM), and the reaction was monitored by following the increase of absorbance at 270 nm where the conjugate of EA with GSH absorbs: $\epsilon_{270} = 5700\ M^{-1}\ cm^{-1}$ (*36*). (2) 0.0025−0.5 mM NBD-Cl in the presence of 0.5 mM GSH in 0.1 M sodium acetate, pH 5.0. The reaction was monitored at 419 nm, $\epsilon = 14\,500\ M^{-1}\ cm^{-1}$ (*37*). Apparent K_m^{GSH} was calculated under the same conditions at fixed NBD-Cl concentration (0.2 mM) and variable GSH concentration (from 0.002 to 0.5 mM). (3) 0.1−2 mM CDNB in the presence of 5 mM GSH in 0.1 M potassium phosphate buffer, pH 6.5, containing 0.1 mM EDTA. The reaction was monitored at 340 nm, $\epsilon = 9600\ M^{-1}\ cm^{-1}$ (*36*). Apparent K_m^{GSH} was also determined at fixed CDNB concentration (1 mM) and variable GSH concentration (from 0.02 to 2 mM). (4) 0.025−0.3 mM 4-nitroquinoline 1-oxide (4-NQO) in the presence of 5 mM GSH in 0.1 M phosphate buffer, pH 6.5. The reaction was monitored at 350 nm, $\epsilon = 7200\ M^{-1}\ cm^{-1}$ (*38*). (5) 0.05−0.8 mM *p*-nitrobenzyl chloride (NBC) in the presence of 5 mM GSH in 0.1 M potassium phosphate buffer, pH 6.5.The reaction was monitored at 310 nm, $\epsilon = 1900\ M^{-1}\ cm^{-1}$ (*36*). Kinetic parameters reported in this paper represent the mean of at least three different experimental data sets.

The pH dependence of k_{cat} and k_{cat}/K_m^{cosub} for different cosubstrates was obtained by using 0.1 M sodium acetate

Table 1: Kinetic Parameters of GST P1-1, Val35Ala, and Val10Gly Mutant Enzymes

substrate	enzyme	K_m^{cosub} (mM^{-1})	K_m^{GSH} (mM^{-1})	k_{cat} (s^{-1})	k_{cat}/K_m^{cosub} (s^{-1} mM^{-1})
EA	WT	0.21 ± 0.02	0.177 ± 0.006	2.57 ± 0.01	12.2 ± 0.8
	Val35Ala	0.145 ± 0.006	0.17 ± 0.01	0.75 ± 0.19	5.17 ± 1.08
	Val10Gly	0.08 ± 0.014	0.1 ± 0.033	0.16 ± 0.03	2 ± 0.1
NBD-Cl	WT	0.004 ± 0.001	0.008 ± 0.002	1.1 ± 0.02	275 ± 12
	Val35Ala	0.012 ± 0.003	0.015 ± 0.006	1.04 ± 0.18	86.6 ± 6
	Val10Gly	0.023 ± 0.008	0.07 ± 0.008	1.65 ± 0.28	71.7 ± 14
CDNB	WT	1.2 ± 0.1	0.15 ± 0.03	76 ± 2	63 ± 2
	Val35Ala	1.55 ± 0.38	0.15 ± 0.038	60 ± 13	38.7 ± 1.25
	Val10Gly	0.45 ± 0.1	0.4 ± 0.025	6.1 ± 2	13.3 ± 3.8
4-NQO	WT	0.33 ± 0.03	nd[a]	73 ± 2	222 ± 20
	Val35Ala	0.38 ± 0.3	nd	40 ± 5	105 ± 18
	Val10Gly	1.25 ± 0.2	nd	3 ± 0.12	2.4 ± 0.023
NBC	WT	0.51 ± 0.12	nd	0.23 ± 0.05	0.45 ± 0.04
	Val35Ala	2.7 ± 0.2	nd	0.75 ± 0.05	0.27 ± 0.015
	Val10Gly	nd	nd	nd	nd

[a]Not determined.

Table 2: Effect of Leaving Group

	GST P1-1 catalyzed reaction	Val10Gly catalyzed reaction
k_{cat}^{FDNB} (s^{-1})	145 ± 0.029	12.8 ± 0.004
k_{cat}^{CDNB} (s^{-1})	76 ± 0.003	6.1 ± 0.02

buffers (from pH 4.0 to pH 5.5) and potassium phosphate buffers (from pH 6.0 to pH 7.5).

Viscosity Variation Experiments. The effect of viscosity on kinetic parameters was assayed by using 0.1 M potassium phosphate and 0.1 M sodium acetate buffers, both containing variable glycerol concentrations. Viscosity values (η) at 25 °C were calculated from the Chemistry Handbook (*39*) and randomly controlled with an Osvald viscosimeter. Viscosities are reported relative to 0.1 M potassium phosphate buffer, pH 6.5, and 0.1 M sodium acetate, pH 5.0.

Thermal Stability. The WT and Val10Gly and Val35Ala mutant enzymes were incubated at different temperatures (range 25−60 °C) for at least 30 min, at a protein concentration of 0.1 mg/mL in 0.1 M phosphate buffer, pH 6.5, containing 0.1 mM EDTA. At regular time intervals, aliquots were withdrawn from the incubation mixture and assayed for GST activity. The results showed that the thermal stability of either Val10Gly and Val35Ala mutant enzymes was unaffected by replacement of Val with Gly or Val with Ala, respectively (data not shown).

Spectroscopic Experiments. The GSH activation by GST P1-1 was followed by difference spectroscopy of the binary complex. GSH (1 mM) was added to 13 μM GST active sites in 1 mL of 0.1 M phosphate buffer, pH 6.5, and the amount of the thiolate formed was monitored between 230 and 310 nm at 25 °C. The resulting spectrum was subtracted from the contribution of either the free enzyme or free GSH. Quantitation of the thiolate was made assuming an $\epsilon_{239} = 5500\ M^{-1}\ cm^{-1}$ (*40*, *41*).

Stopped-Flow Analysis. Rapid kinetic experiments were performed on an Applied Photophysics kinetic spectrometer stopped-flow instrument equipped with a temperature-regulated observation chamber, a 1 cm light path, and 1 ms dead time. In a typical experiment, WT (66 μM), or Val10Gly (60 or 114 μM), in 0.1 M potassium phosphate buffer, pH 6.5, containing GSH at the following concentrations, 10, 4, or 0.5 mM, was mixed with 2 mM CDNB or 0.6 mM EA dissolved in the same buffer. The reaction was followed spectrophotometrically at 340 or 270 nm and at different temperatures (between 4 and 25 °C). The time course of the product (P) formation was fitted to the equation:

$$[P] = [E_0](k_1/(k_1 + k_2))^2 - [E_0](k_1/(k_1 + k_2))^2 \exp(-(k_1 + k_2)t) + [E_0](k_1/(k_1 + k_2))k_2t \quad (1)$$

which gives the pseudo-first-order rate constant for the formation of the product (k_1) and the first-order rate constant for the release of product from the active site (k_2) (*42*).

Effect of Temperature on the GSH Conjugation with CDNB or EA. The dependence of reaction rate against temperature was evaluated by measuring k_{cat} at different temperature values (4−35 °C) under the same conditions reported above. The activation energy was calculated by plotting log k_{cat} versus $1/T$.

Crystallization. Crystallization was performed by the hanging drop vapor diffusion method as described elsewhere (*23*). Briefly, a 2 μL drop of a 9.5 mg/mL protein solution containing 10 mM phosphate buffer (pH 7.0), 0.1 mM EDTA, and 2 mM mercaptoethanol was mixed with an equal volume of reservoir solution which consisted of 20−25% (w/v) ammonium sulfate, 50−60 mM DTT, 100 mM MES buffer (pH range 5.0−5.4), and 10 mM *S*-hexyl-GSH (which was synthesized according to the method given in ref *43*). All trials were carried out at a constant temperature of 22 °C, and crystals took between 1 and 4 days to appear and grew to final size in about 1 week.

X-ray Data Collection. The X-ray diffraction data were collected using a MARResearch area detector with Cu Kα X-rays generated by a Rigaku RU-200 rotating anode X-ray generator. The data were collected at room temperature. Data from a number of flash-frozen crystals were also collected. However, these flash-frozen data sets would not refine satisfactorily despite exhibiting better data collection statistics than the room temperature data set (unpublished results). Diffuse scattering could be observed in the diffraction pattern of the frozen crystals whereas none was observed for the room temperature crystals. It thus appears that flash-freezing introduced static disorder in the crystals. The diffraction data were processed and analyzed using programs in the HKL (*44*) and CCP4 (*45*) suites. The relevant data statistics are presented in Table 4.

Model Building and Refinement. Refinement began with the model of the *S*-hexyl-GSH complex in the C2 group (9GSS; *23*) which had inhibitor and water molecules

Table 3: Temperature Dependence of Kinetic Parameters in the Enzymatic Conjugation with CDNB[a]

temp (°C)	Val10Gly		temp (°C)	Val10Gly	
	k_1 (s^{-1})	k_2 (s^{-1})		k_1 (s^{-1})	k_2 (s^{-1})
4	1.63	0.46	16	6.87	3.23
8	2.87	0.86	21	8.5	7.68
12	4.3	1.57	25	8.4	7.8

[a] k_1 is the pseudo-first-order rate constant for the formation of the product, and k_2 is the first-order rate constant for the release of product from the active site (see Scheme 1). The values of these constants obtained at different temperatures are calculated from the best fit of experimental data according to eq 1 (see Experimental Procedures).

Table 4: Data Collection and Processing for Val10Gly

temp (K)	298	no. of observations	41673
space group	$P4_32_12$	no. of unique reflns	11101
cell dimensions		data completeness (%)	94
a, *b* (Å)	60.1	completeness $>2\sigma_I$ (%)	72
c (Å)	239.6	I/σ_I	13.4
max resoln (Å)	2.8	multiplicity	3.8
no. of crystals	1	R_{merge}[a] (%)	10.3

[a] $R_{merge} = \sum_{hkl}\sum_i |I_i - \langle I\rangle|/|\langle I\rangle|$, where I_i is the intensity for the *i*th measurement of an equivalent reflection with indices *h*,*k*,*l*.

Table 5: Refinement Statistics for Val10Gly

non-hydrogen atoms	
protein	3270
inhibitor	52
solvent	74
resolution (Å)	2.8
R_{conv} (%)	23.7
R_{free} (%)	28.7
reflns used in R_{conv} and R_{free} calcns	
work set	9974
test set	972
rmsds from ideal geometry	
bonds (Å)	0.009
angles (deg)	1.28
dihedrals (deg)	20.4
impropers (deg)	0.77
bonded B's ($Å^2$)	2.04
residues in most favored regions of Ramachandran plot (%)	89.6

removed. Rigid body refinement in CNS (*46*) was used to compensate for any possible changes in crystal packing. As the asymmetric unit of the crystal contained two GST monomers, noncrystallographic symmetry (NCS) restraints were used throughout the course of refinement. A bulk solvent correction was employed during refinement. Typically, a number of rounds of positional refinement were performed interspersed by model building and then followed by rounds of positional and individual NCS-restrained *B*-factor refinement. The inhibitor and water molecules were fitted into the maps in the final rounds. For *S*-hexyl-GSH, bond lengths and angles were taken from the PDB entry 9GSS (*23*). In the A monomer no density was observed for the hexyl tail whereas in the B monomer weak but continuous density was observed (when contoured at 0.8σ) for the C2 to C6 portion of the tail. The fit of the inhibitor into the final electron density map is shown in Figure 7. The final refinement statistics are presented in Table 5. A stereochemical analysis of the refined structure with the program PROCHECK (*47*) gave values either similar or better than expected for structures refined at similar resolutions.

RESULTS

Kinetic Analysis of the WT and Mutant Enzymes. The replacement of Val 35 to Ala and Val 10 to Gly was done by site-directed mutagenesis, and both proteins were successfully expressed in *E. coli* cells and purified according to a standard procedure (*31*).

Steady-state kinetic analysis of the Val35Ala mutant using a number of selected cosubstrates shows no substantial differences with respect to the native enzyme (Table 1). In fact, in the enzymatic conjugation of GSH with EA or with 4-NQO there is only a slight decrease of 3- and 2-fold of the k_{cat} values, respectively. With NBD-Cl and NBC as cosubstrates there is instead a 3- and 5-fold increase of the K_m values, respectively, and a 3-fold increase of the k_{cat} value for NBC. No significant differences are found in the kinetic parameters between this mutant enzyme and the WT with CDNB as cosubstrate.

The replacement of Val 10 to Gly greatly affects the catalytic properties of GST P1-1. Except in the case of NBD-Cl, there is a general and significant decrease of k_{cat} values toward a number of selected cosubstrates (Table 1). For example, the k_{cat} values for the enzymatic conjugation of GSH with EA, CDNB, or 4-NQO are 16-, 12-, and 24-fold less than that of WT, respectively. The changes of K_m values are also noticeable and vary according to the selected cosubstrate. In the conjugation of NBD-Cl there is a large increase of the K_m values for both substrates (GSH and NBD-Cl), suggesting a decreased affinity of the mutant enzyme for these substrates as the main effect of this point mutation. There is also a 4-fold higher value of the K_m value for 4-NQO as cosubstrate. In contrast, for EA and CDNB there is a slight decrease of K_m values. We decided to further investigate the effect of this mutation using CDNB and EA as cosubstrates because both are commonly used substrates for Pi class GSTs.

Effect of Replacement of Val 10 with Gly in the Enzymatic Conjugation with CDNB. This is the first residue of GST P1-1 so far investigated, apart from Tyr 7, which produces a significant decrease of the k_{cat} value in the nucleophilic aromatic substitution reaction with CDNB (Table 1). Despite the apolar character of its side chain, its close location to Tyr 7 prompted us to investigate whether it could influence the activation of the GSH substrate bound to the enzyme in the binary complex. The dependence of kinetic parameters on pH in the binary complex (Figure 1B) yielded a pK_a value of 6.1 $\pm$ 0.1, a value very close to that found in the WT enzyme (6.2 $\pm$ 0.08), suggesting that the ionization process of GSH is unaffected by this point mutation. Direct evidence for this was also gained by spectroscopic measurement of the thiolate anion of GSH (*40*, *41*) complexed in the active site of the V10G mutant: the extent of the thiolate species is very similar to that of the WT (data not shown). A pH dependence of k_{cat} in the ternary complex of the mutant enzyme is slightly different from that of WT and identifies a pK_a of 5.18 $\pm$ 0.16 instead of 6.2 $\pm$ 0.08 obtained for the WT (Figure 1A).

We have previously suggested that in the GSH−CDNB conjugation reaction catalyzed by GST P1-1 the rate-limiting step may be some structural transitions which occur after binding of substrates and before the chemical event (σ complex formation) (*48*). Steady-state kinetic experiments

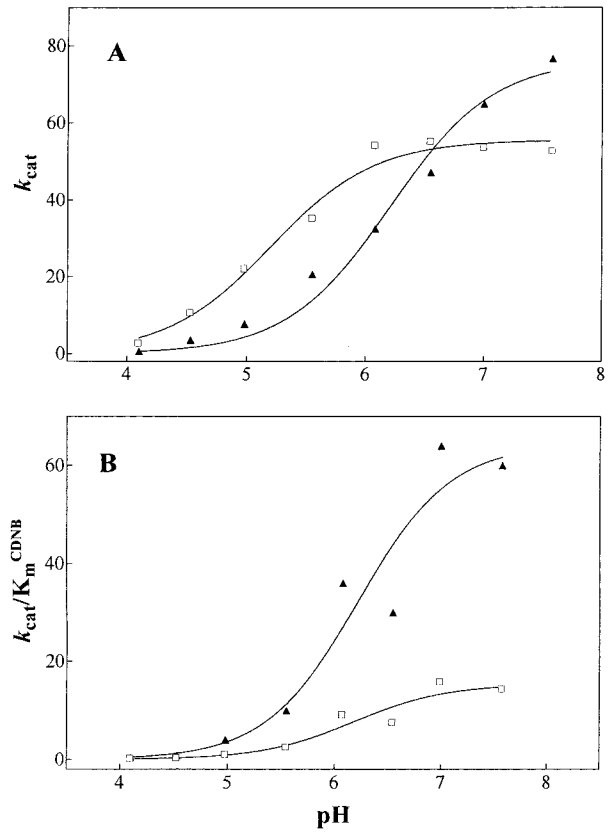

FIGURE 1: pH dependence of kinetic parameters for CDNB−GSH conjugation. The solid lines are computer fits of the experimental data with GST P1-1 (▲) and Val10Gly (□) to the equations $k_{cat} = k_{cat}^{lim}/(1 + 10^{-pH}/K_a)$ (panel A) and $k_{cat}/K_m^{CDNB} = (k_{cat}/K_m^{CDNB})^{lim}/(1 + 10^{-pH}/K_a)$ (panel B). The pH values measured are within the pH 4.0−8.0 range. The pK_a values in panel A, calculated by fits, are 5.18 for Val10Gly and 6.2 for WT, and the k_{cat} values for the Val10Gly mutant are multiplied 10-fold to facilitate comparison with those of the WT enzyme. The pK_a values in panel B are 6.18 and 6.2, respectively, for Val10Gly and WT.

of Val10Gly and WT enzymes carried out in the presence of glycerol suggest that in both cases k_{cat} is diminished by about three times in the mutant (Figure 2). The effect of the leaving group on the turnover number was also examined using FDNB (where fluoride replaces the chloride atom of CDNB) as cosubstrate. The results clearly show that k_{cat} in the Va10Gly mutant is insensitive to the chemical event (Table 2). Thus it appears that, for both WT and Val10Gly, a physical event governs the rate-limiting step of this reaction. We therefore investigated whether this physical process should be related to the structural transitions referred to above or product release by performing pre-steady-state kinetic experiments (stopped-flow kinetics). The results obtained at 4 °C show a burst phase at 340 nm, suggesting that the dinitrophenylglutathione (DNP-GSH) accumulated before steady-state conditions are attained (Figure 3A). However, when the same experiment was repeated at higher temperature values, the burst phase was diminished, and at 21 °C, it was difficult to distinguish between the values of k_1 and k_2 (Figure 3B and Table 3; see also Scheme 1). These results suggest that there may be a change of the rate-limiting step with temperature.

An Arrhenius plot showing the dependence of k_{cat} on the temperature for the Val10Gly mutant was also calculated and compared to that of WT (Figure 4). A fitting of

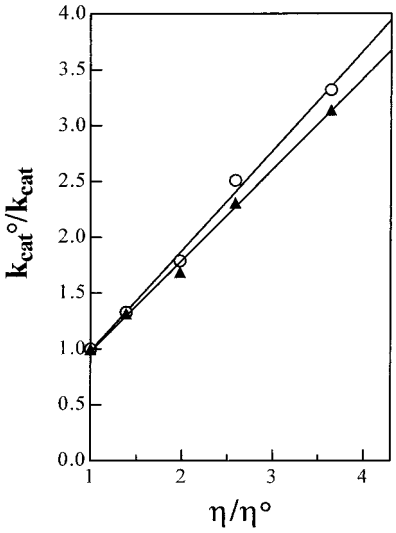

FIGURE 2: Viscosity effect on kinetic parameters of WT and Val10Gly mutant enzymes. Dependence of the reciprocal of the relative turnover numbers ($k_{cat}°/k_{cat}$) on the relative viscosity ($\eta/\eta°$) for CDNB as cosubstrate with WT (▲) and Val10Gly (○) mutant enzymes. Kinetic data for enzymatic reactions were obtained as described in Experimental Procedures. Slopes of linear fits are 0.81 and 0.89 with WT and Val10Gly mutant enzymes, respectively.

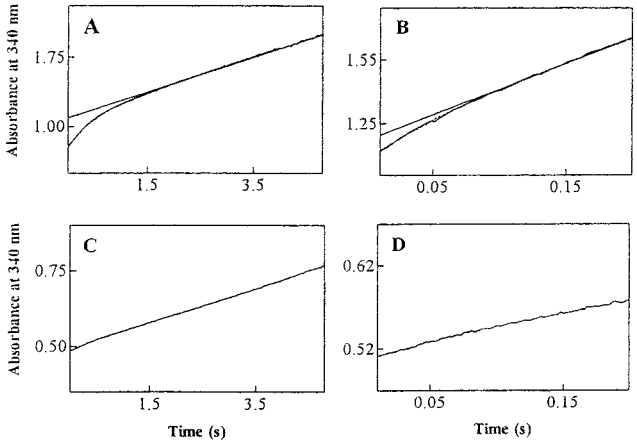

FIGURE 3: Time course of the enzymatic GS−CDNB production. Kinetics were obtained by mixing in a stopped-flow apparatus the WT (16 μM) and the Val10Gly mutant enzyme (114 μM), respectively, in 0.1 M potassium phosphate buffer, pH 6.5, containing 10 mM GSH, with 2 mM CDNB in the same buffer. Panels: A, Val10Gly at 4 °C; B, Val10Gly at 21 °C; C, WT at 4 °C; D, WT at 21 °C. The continuous lines represent the best fit of the data to eq 1, whereas the straight lines represent the linear portion extrapolated back to the burst value (panels A and B).

experimental data to straight lines (from 4 to 35 °C) indicates the presence of two slopes with two different activation energy values calculated: the first one is of 43.65 ± 1.3 kJ/mol, a value close to that of WT (58.5 ± 1.38 kJ/mol), and the second displays a doubled activation energy value (99 ± 0.44 kJ/mol) and is in the same range of temperature where a burst phase is clearly observed under pre-steady-state conditions (Figure 3A). Under these latter conditions, by plotting log k_2 versus temperature, we determined also a value of 114 ± 0.47 kJ/mol as activation energy, which is in agreement with the value reported under steady-state

Scheme 1

$$E + GSH + CDNB \xrightarrow{k_1} EP \xrightarrow{k_2} E + P$$

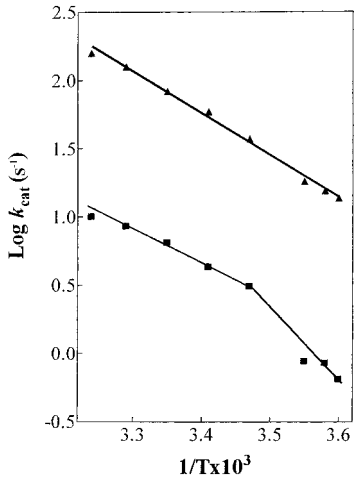

FIGURE 4: Temperature effect on kinetic parameters in the GSH−CDNB conjugation reaction. The Arrhenius plots, obtained between 4 and 35 °C, show the different behavior exhibited by WT (▲) and Val10Gly (■) mutant enzymes, respectively.

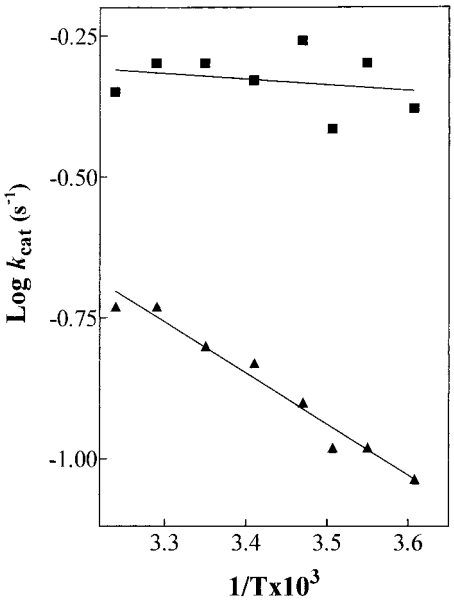

FIGURE 5: Temperature effect on kinetic parameters in the EA−GSH conjugation reaction. The Arrhenius plots, obtained between 4 and 35 °C, show the different behavior exhibited by WT (■) and Val10Gly (▲) mutant enzymes, respectively.

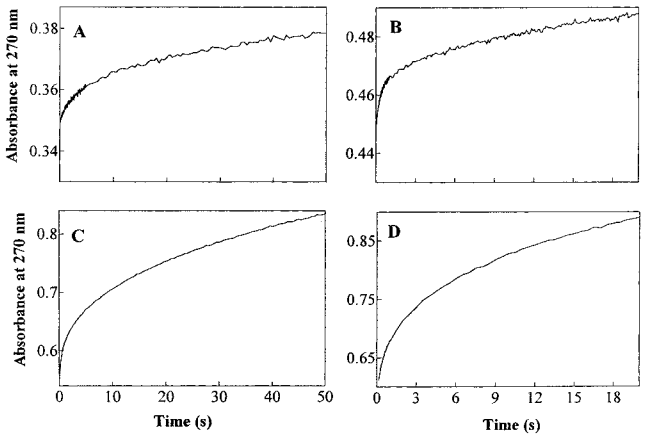

FIGURE 6: Time course of the enzymatic GS−EA production. Kinetics were obtained by mixing in a stopped-flow apparatus WT (60 μM) and the Val10Gly mutant enzyme (60 μM), respectively, in 0.1 M potassium phosphate buffer, pH 6.5, containing 0.5 mM GSH, with 0.6 mM EA in the same buffer. Panels: A, Val10Gly at 6 °C; B, Val10Gly at 25 °C; C, WT at 6 °C; D, WT at 25 °C. The curves represent only the traces obtained by the stopped-flow apparatus.

conditions at low-temperature range (Figure 4) and is what is expected assuming that k_2 and k_{cat} are the same constant. Therefore, the Arrhenius plot at steady-state level confirms what is suggested by stopped flow-experiments: a change in the rate-limiting step of the reaction with temperature. According to these results the transition temperature is about 15 °C. At temperature values below 15 °C the rate-limiting step may be related to a product release while above this temperature the rate-limiting step is associated with structural transitions already described for the WT (*48*).

Effect of Replacement of Val 10 with Gly in the Enzymatic Conjugation with EA. As seen in Table 1 the most dramatic effect observed with the Val10Gly mutant, in the enzymatic conjugation with EA, is a large decrease of the k_{cat} value. We have previously suggested that, in the WT enzyme, the kinetic mechanism for the enzymatic conjugation between GSH and EA involves a rapid equilibrium (*27*). Therefore, the fact that, in the mutant, K_m values for both substrates are substantially unchanged while the catalytic efficiency k_{cat}/K_m^{EA} is lowered ruled out the possibility that this mutation would cause a nonproductive binding of either GSH or EA at the active site in the ternary complex. The pH dependence of k_{cat}/K_m^{EA} in the binary complex (GSH−enzyme) and of k_{cat} in the ternary complex (GSH−enzyme−EA) is unaffected by this point mutation since both are similar to those of the WT enzyme (data not shown). Quite unexpectedly, we observed a strong dependence of k_{cat} on the temperature, in the range of 4−35 °C, in contrast to the behavior of the WT enzyme, which appears to be much less sensitive to the temperature (see the Arrhenius plot of Figure 5). In fact, the corresponding activation energy values calculated are 17.2 ± 0.067 kJ/mol and 1.91 ± 0.15 kJ/mol for the Val10Gly mutant and WT enzymes, respectively. This significant difference in the activation energy may be indicative of a change in the rate-limiting step of this reaction. We have previously suggested that in the catalyzed GSH conjugation with EA the rate-limiting step could be the chemical event of the Michael addition of GSH to EA for the WT enzyme (*27*). Now, by performing stopped-flow experiments with both WT and Val10Gly mutant enzymes, we have obtained new data which shed more light on the catalytic mechanism of GSH conjugation with EA. In fact, pre-steady-state kinetics of both WT and Val10Gly mutant enzymes shows a burst phase over a wide range of temperature (from 6 to 25 °C) (see Figure 6A,B) and suggests that the product release of the EA−GSH conjugate is the rate-limiting step. We cannot produce a reliable and accurate fitting of these curves to get the corresponding constants (k_1 and k_2) because the chemical event (product formation) is partially localized within the instrument dead time and also influenced by an overcoming product inhibition. However, as a rough estimate, we observe that k_1 is substantially unchanged while k_2 is diminished by about 20 times in the mutant, in comparison with the WT enzyme.

Crystallographic Analysis of the V10G Mutant Enzyme. The initial electron density map was of sufficient quality to demonstrate the lack of any significant conformational changes to the enzyme caused by replacement of the valine

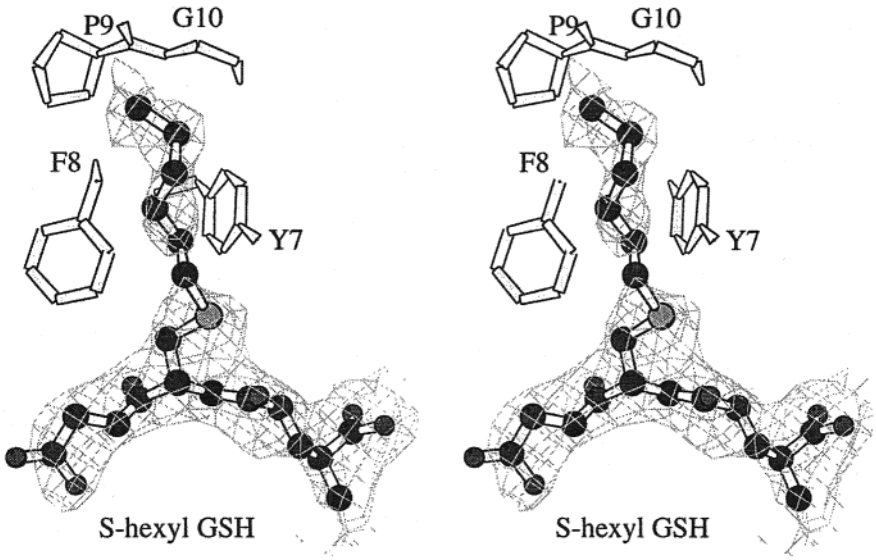

FIGURE 7: Stereo diagram of the final $2F_o - F_c$ electron density map of the *S*-hexyl-GSH complex in the vicinity of the inhibitor binding site of the B monomer of human Val10Gly GST P1-1. The map was calculated using all reflections and contoured at the 0.8σ level.

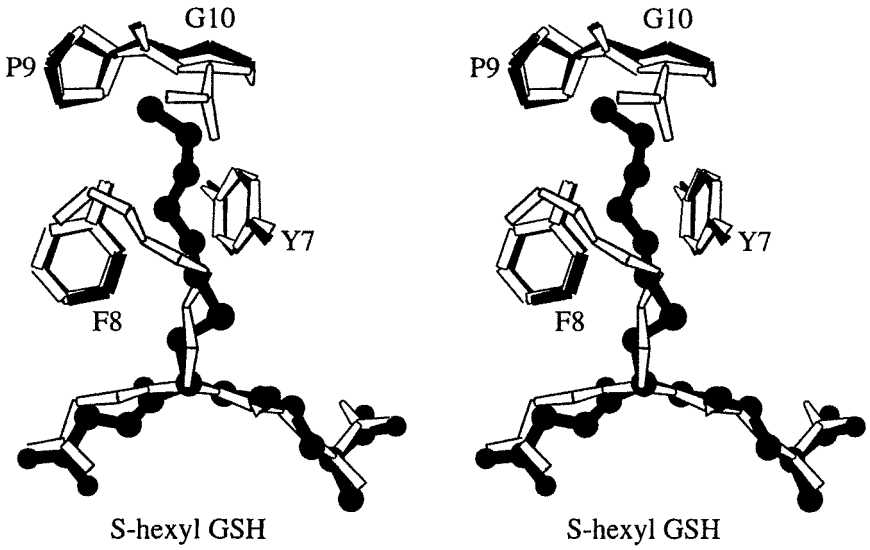

FIGURE 8: Superposition of wild-type (hollow bonds) and Val10Gly *S*-hexyl-GSH complex (filled bonds) structures in the vicinity of the active site of the B monomer.

except for a small movement (0.8 Å) of the replaced residue toward Leu 201 of the C-terminal tail of the enzyme (Figure 8). Residue 10 forms part of the floor of the H-site, and the mutation causes the floor to be slightly lowered. Among the significant features in the initial difference electron density map were negative peaks (approximately 3σ) over the position of the Val 10 side chain in each monomer, thus confirming the mutation. The protein and GSH components of the *S*-hexyl-GSH Val10Gly GST P1-1 complex and the *S*-hexyl-GSH WT GST P1-1 complex (9GSS; *23*) have almost identical structures. The root-mean-square deviation in α-carbon positions is 0.36 Å with no movements greater than 1 Å. The ϕ, ψ angles for Gly 10 are 179° and 174°, respectively, compared to wild-type values of −145° and 164°. Any other residue which adopted the same ϕ, ψ angles as the glycine could not be accommodated without conformational changes because the side chain would sterically clash with Pro 202.

In the Val10Gly complex, electron density for the hexyl tail is not observed at all in the A monomer but weak, continuous density over the C2 to C6 atoms is observed in the B monomer. In the $P4_32_12$ space group the regions about the H-site are involved in crystal contacts in both monomers. Presumably the observation of the hexyl tail in only one monomer is due to these crystal contacts. In the A monomer there are crystal contacts with helix α2 which borders the G-site and provides only one or two residues to the H-site. In contrast, there are many more crystal contacts in the region around the H-site in the B monomer. The contacts include multiple hydrogen bonding and van der Waals interactions with the C-terminal tail that forms part of a wall to the H-site and also a van der Waals contact with the α1 strand−α1 helix loop in which residue 10 is located. The hexyl tail in the B monomer points toward the β1 strand−α1 helix loop (residues 8−14) with the C5 and C6 atoms close to the position where the Val 10 side chain used to be located. The tail is found resting against the floor of the H-site and makes van der Waals contacts with Tyr 7, Phe 8, Pro 9, and Gly 10. Although the hexyl tail in the wild-type structure also interacts with the aromatic rings of Tyr 7 and Phe 8, it heads

off in a different direction (Figure 8), pointing toward the C-terminus and making van der Waals interactions with Val 35 and Gly 205. Thus, although Val 10 does not interact with the hexyl tail in the wild-type structure, it is responsible for directing the tail toward the C-terminus of the enzyme and stabilizing its position (since the tail is not observed in one monomer of the mutant and only weakly in the other monomer).

DISCUSSION

Mutagenesis studies on different GSTs have shown that profound differences in the enzymatic activities toward certain substrates depend essentially on a single or very few amino acid residues. This has been clearly demonstrated for some mammalian Alpha class isoenzymes (*49*−*51*) and is becoming apparent for Pi class GSTs. Recent studies on class Pi polymorphism pointed out the importance of some residues located into the H-site. For example, two different laboratories reported the expression in mouse of two GST Pi genes which differ only in six amino acids (*52*, *53*). Two of these substitutions are located in the N-terminal domain (Val 10 and Arg 11) and are believed to be responsible for the reduced activity of the mutated gene (*54*). In the human GST P1-1, Ali-Osman and colleagues (*55*) have described the presence of three mutations at positions 104 and 113 and their effect on the enzymatic activity. The results of the present paper confirm the importance of Val 10 in catalysis with a number of cosubstrates (see Table 1). In contrast, Val 35, a residue not conserved among the isoenzymes of the same class, is shown to be not important with these substrates because the mutant Val35Ala behaves like the WT. Shan and Armstrong have suggested that, in the rat class Mu 4-4, Val9Ile mutation (Val 9 being the counterpart of Val 10 in class Mu) is involved in the stereoselectivity toward enones and epoxides (*56*).

The overall effect of the Val10Gly mutation is a strong decrease of the k_{cat} values and the catalytic efficiencies with both substrates (CDNB or EA), irrespective of the different chemical mechanisms (i.e., the nucleophilic aromatic substitution with CDNB and the Michael addition with EA) on which these reactions rely. The kinetic data with NBD-Cl are in apparent contrast to those of CDNB and EA. We have previously shown that NBD-Cl is a poor substrate of GST P1-1 with the conjugation reaction being rate-limited by a slow and non-diffusion-controlled motion of an active site helix (*57*). This high-energy barrier, which was not observed in the other cosubstrates, would mask any effects induced by the Val10Gly mutation. In the case of EA as cosubstrate, a detailed kinetic analysis of the Val10Gly mutant, at steady-state level, reveals that this k_{cat} decrease is related to a significant increase of the activation energy (about 17-fold as compared with that of WT; see Figure 5). Stopped-flow kinetic analysis, carried out in the same range of temperature, shows a burst phase in both WT and Val10Gly mutant enzymes and indicates that the dissociation of the product as the rate-limiting step is unchanged in the mutant enzyme. However, the mutation has caused an increase of the energetic barrier in the dissociation of the product from the active site. On the basis of these results the effect of this point mutation can be explained in at least two different ways: (1) a change in structural flexibility of the H-site or (2) if Val 10 is a guide for the exit of products from the active site, its removal lowers the overall turnover rate. Similar explanation can be made about the removal of this residue in the enzymatic conjugation with CDNB at temperatures below 15 °C, where the rate-limiting step is product release. However, with this cosubstrate we observe an additional role of Val 10: at temperatures higher than 15 °C it influences also the structural transitions of the ternary complex before the chemical event.

Despite considerable efforts, we have not been able to obtain crystals of the Val10Gly mutant complexed with GS−EA or DNP-GSH. However, a comparison of the structures of the Val10Gly mutant complexed with *S*-hexyl-GSH and the equivalent WT complex is still informative as it provides clues as to the structural basis of the observed changes in the catalysis. The apolar character of its side chain rules out the possibility that Val 10, located at the bottom of the H-site, is involved in the chemical step of either reaction (i.e., the nucleophilic aromatic substitution with CDNB and the Michael addition with EA) as already seen for Tyr 108 (*27*) in the GSH conjugation with EA. Nonetheless, the same side chain could establish some van der Waals contacts with the cosubstrate (CDNB or EA), which may be relevant for the optimal positioning of either cosubstrate and/or the exit of products from the H-site. In fact, the crystallographic data presented here indicate that the absence of this side chain in the Val10Gly mutant renders the hexyl tail of the inhibitor more flexible where in one monomer it is not observed at all and in the other it is only weakly observed. This tail now points toward the β1 strand−α1 helix loop while in the presence of Val 10 it is directed toward the C-terminus (*23*). There are only a few changes in the van der Waals contacts between the hexyl tail and residues nearby: the contacts with Tyr 7 and Phe 8 remain unchanged but those with Val 35 and Gly 205 are replaced with Pro 9 and Val10Gly, respectively, due to the altered direction of the hexyl tail. Previous crystallographic results have demonstrated at least two different binding modes of the product (GSH conjugates) in the H-site: mode IN and mode OUT (*26*, *58*). In the previously published structures of GS−EA bound in either IN mode (*59*) or OUT mode (*24*), Val 10 is within van der Waals distance of the EA moiety. A structure of 1,3,5-trinitrobenzene GSH bound to the Pi class enzyme (a model for a transition state σ-complex) shows that it binds in the IN mode (*22*) while the product (DNP-GSH) binds in the OUT mode (*26*). In these structures Val 10 is within van der Waals distance of the aromatic ring in the former but is more than 8 Å away in the latter. The contribution of Val 10 to product release probably occurs in the transition from the IN to OUT modes, and such a dynamic process cannot be observed crystallographically. However, a number of previous studies on GST P1-1 have demonstrated the importance of active site dynamics toward understanding the kinetic behavior of the enzyme (*48*, *60*−*63*). Therefore, altogether these kinetic and crystallographic results are consistent with our proposal that Val 10 plays a role in promoting the exit of products from the active site.

In a previous study on the mutated gene of mouse GST Pi (GSTp-2) Bammler et al. (*54*) mutated Val 10 into serine to study the contribution of this single mutation to the reduced activity exhibited by this gene. They found a 5-fold decrease of the k_{cat} value with CDNB as cosubstrate and no significant change in K_m for either CDNB or GSH. The

results of the present paper, obtained by mutating Val 10 of the human enzyme into glycine, are consistent with these data, and our work may provide a molecular basis for understanding the effects observed in both enzymes.

ACKNOWLEDGMENT

We are indebted to Prof. Massimo Coletta, University of Rome Tor Vergata, for helpful discussions and assistance with the stopped-flow apparatus.

REFERENCES

1. Jakoby, W. B., and Habig, W. H. (1980) in *Enzymatic Basis of Detoxification* (Jakoby, W. B., Ed.) Vol. 2, pp 63−94, Academic Press, New York.
2. Mannervik, B., Ålin, P., Guthenberg, C., Jensson, H., Tahir, M. K., Warholm, M., and Jörnvall, H. (1985) *Proc. Natl. Acad. Sci. U.S.A. 82*, 7202−7206.
3. Meyer, D. J., Coles, B., Pemble, S. E., Gilmore, K. S., Fraser, G. M., and Ketterer, B. (1991) *Biochem. J. 274*, 409−414.
4. Buetler, T. M., and Eaton, D. L. (1992) *Environ. Carcinog. Ecotoxicol. Rev. 10*, 181−200.
5. Ji, X., von Rosenvinge, E. C., Johnson, W. W., Tomarev, S. I., Piatigorsky, J., Armstrong, R. N., and Gilliland, G. L. (1995) *Biochemistry 34*, 5317−5328.
6. Pemble, S. E., Wardle, A. F., and Taylor, J. B. (1996) *Biochem. J.* 319, 749−754.
7. Board, P. G., Baker, R. T., Chelvanayagam, G., and Jermiin, L. S. (1997) *Biochem. J. 328*, 929−935.
8. Rossjohn, J., Polekhina, G., Feil, S. C., Allocati, N., Masulli, M., Di Ilio, C., and Parker, M. W. (1998) *Structure 6*, 721−734.
9. Armstrong, R. N. (1997) *Chem. Res. Toxicol. 10*, 2−18.
10. Mannervik, B., Awasthi, Y. C., Board, P. G., Hayes, J. D., Di Ilio, C., Ketterer, B., Listowsky, I., Morgerstern, R., Muramatsu, M., Pearson, W. R., Pickett, C. B., Sato, K., Widersten, M., and Wolf, C. R. (1992) *Biochem. J. 282*, 305−308.
11. Kano, T., Sakai, M., and Muramatsu, M. (1987) *Cancer Res. 47*, 5626−5630.
12. Tsuchida, S., Sekine, Y., Shineha, R., Nishihira, T., and Sato, K. (1989) *Cancer Res. 49*, 5225−5229.
13. Batist, G., Tulpule, A., Sinha, B. K., Katki, A. G., Myers, C. E., and Cowan, K. H. (1986) *J. Biol. Chem. 261*, 15544−15549.
14. Black, S. M., Beggs, J. D., Hayes, J. D., Bartoszek, A., Muramatsu, M., Sakai, M., and Wolf, C. R. (1990) *Biochem. J. 268*, 309−315.
15. Puchalski, R., and Fahl, W. E. (1990) *Proc. Natl. Acad. Sci. U.S.A. 87*, 2443−2447.
16. Adler, V., Yin, Z., Fuchs, S. Y., Benezra, M., Rosario, L., Tew, K. D., Pincus, M. R., Sardana, M., Henderson, C. J., Wolf, C. R., Davis, R. J., and Ronai, Z. (1999) *EMBO J. 18*, 1321−1334.
17. Piredda, L., Farrace, M. G., Lo Bello, M., Malorni, W., Melino, G., Petruzzelli, R., and Piacentini, M. (1999) *FASEB J. 13*, 355−364.
18. Kong, K. H., Inoue, H., and Takahashi, K. (1992) *J. Biochem. 112*, 725−728.
19. Manoharan, T. H., Gulick, A. M., Reinemer, P., Dirr, H. D., Huber, R., and Fahl, W. H. (1992) *J. Mol. Biol. 226*, 319−322.
20. Reinemer, P., Dirr, H. W., Ladenstein, R., Huber, R., Lo Bello, M., Federici, G., and Parker, M. W. (1992) *J. Mol. Biol. 227*, 214−226.
21. Widersten, M., Kolm, R. H., Bjornstedt, R., and Mannervik, B. (1992) *Biochem. J. 285*, 377−381.
22. Prade, L., Huber, R., Manoharan, T. H., Fahl, W. E., and Reuter, W. (1997) *Structure 5*, 1287−1295.
23. Oakley, A. J., Lo Bello, M., Battistoni, A., Ricci, G., Rossjohn, J., Villar, H. O., and Parker, M. W. (1997) *J. Mol. Biol. 274*, 84−100.
24. Oakley, A. J., Rossjohn, J., Lo Bello, M., Caccuri, A. M., Federici, G., and Parker, M. W. (1997) *Biochemistry 36*, 576−585.
25. Ji, X., Tordova, M., O'Donnell, R., Parsons, J. F., Hayden, J. B., Gilliland, G. L., and Zimniak, P. (1997) *Biochemistry 36*, 9690−9702.
26. Oakley, A. J., Lo Bello, M., Nuccetelli, M., Mazzetti, A. P., and Parker, M. W. (1999) *J. Mol. Biol. 291*, 913−926.
27. Lo Bello, M., Oakley, A. J., Battistoni, A., Mazzetti, A. P., Nuccetelli, M., Mazzarese, G., Rossjohn, J., Parker, M. W., and Ricci, G. (1997) *Biochemistry 36*, 6207−6217.
28. Zimniak, P., Nanduri, B., Pikula, S., Bandorowicz-Pikula J., Singhal, S. S., Srivastava, S. K., Awasthi, S., and Awasthi, Y. C. (1994) *Eur. J. Biochem. 224*, 893−899.
29. Johansson, A. S., Stenberg, G., Widersten, M., and Mannervik, B. (1998) *J. Mol. Biol. 278*, 687−698.
30. Battistoni, A., Mazzetti, P., Petruzzelli, R., Muramatsu, M., Ricci, G., Federici, G., and Lo Bello, M. (1995) *Protein Exp. Purif. 6*, 579−587.
31. Lo Bello, M., Battistoni, A., Mazzetti, A. P., Board, P. G., Muramatsu, M., Federici, G., and Ricci, G. (1995) *J. Biol. Chem. 270*, 1249−1253.
32. Kunkel, T. A., Bebenek, K., and McClary, J. (1990) *Methods Enzymol. 204*, 125−139.
33. Simmons, P. C., and Van der Jagt, D. L. (1977) *Anal. Biochem. 82*, 334−341.
34. Laemmli, U. K. (1970) *Nature 227*, 680−685.
35. Lowry, O. H., Rosebrough, N. J., Farr, A. L., and Randall, R. J. (1951) *J. Biol. Chem. 193*, 265−275.
36. Habig, W. H., Pabst, M. T., and Jakoby, W. B. (1974) *J. Biol. Chem. 249*, 7130−7139.
37. Ricci, G., Caccuri, A. M., Lo Bello, M., Pastore, A., Piemonte, F., and Federici, G. (1994) *Anal. Biochem. 218*, 463−465.
38. Stanley, J. S., and Benson, A. M. (1988) *Biochem. J. 256*, 303−306.
39. Wolf, A. V., Brown, M. G., and Prentiss, P. G. (1985) in *Handbook of Chemistry and Physics* (Weast, R. C., Astle, M. J., and Beyer, W. H., Eds.) pp D219−D269, CRC Press, Inc., Boca Raton, FL.
40. Armstrong, R. N. (1991) *Chem. Res. Toxicol. 4*, 131−139.
41. Caccuri, A. M., Lo Bello, M., Nuccetelli, M., Nicotra, M., Rossi, P., Antonini, G., Federici, G., and Ricci, G. (1998) *Biochemistry 37*, 3028−3034.
42. Fersht, A. (1985) *Enzyme Structure and Mechanism*, 2nd ed., W. H. Freeman and Co., New York.
43. Parker, M. W., Lo Bello, M., and Federici, G. (1990) *J. Mol. Biol. 213*, 221−222.
44. Otwinowski, Z. (1993) in *Data Collection and Processing* (Sawyer, L., Isaacs, N., and Bailey, S., Eds.) pp 56−62, SERC Daresbury Laboratory, Warrington, U.K.
45. CCP4 (1994) *Acta Crystallogr., Sect. D 50*, 750−763.
46. Brünger, A. T., Kuriyan, J., and Karplus, M. (1987) *Science 235*, 458−460.
47. Laskowski, R. A., McArthur, M. W., Moss, D. S., and Thorton, J. M. (1993) *J. Appl. Crystallogr. 26*, 282−291.
48. Ricci, G., Caccuri, A. M., Lo Bello, M., Rosato, N., Mei, G., Nicotra, M., Chiessi, E., Mazzetti, A. P., and Federici, G. (1996) *J. Biol. Chem. 271*, 16187−16192.
49. Bjornestedt, R., Tardioli, S., and Mannervik, B. (1995) *J. Biol. Chem 270*, 29705−29709.
50. Xia, H., Gu, Y., Pan, S., Ji, X., and Singh, S. (1999) *Biochemistry 38*, 9824−9830.
51. Nanduri, B., and Zimniak, P. (1999) *Arch. Biochem. Biophys. 362*, 167−174.
52. Bammler, T. K., Smith, C. A. D., and Wolf, C. R. (1994) *Biochem. J. 298*, 385−390.
53. Xu, X., and Stambrook, P. J. (1994) *J. Biol. Chem. 269*, 30268−30273.
54. Bammler, T., Driessen, H., Finnstrom, N., and Wolf, C. R. (1995) *Biochemistry 34*, 9000−9008.
55. Ali-Osman, F., Akande, O., Antoun, G., Mao, J. X., and Boulamwini, J. (1997) *J. Biol. Chem. 15*, 10004−10012.
56. Shan, S., and Armstrong, R. N. (1994) *J. Biol Chem. 269*, 32373−32379.

57. Caccuri, A. M., Ascenzi, P., Antonini, G., Parker, M. W., Oakley, A. J., Chiessi, E., Nuccetelli, M., Battistoni, A., Bellizia, A., and Ricci, G. (1996) *J. Biol. Chem. 271*, 16193−16198.
58. Ji, X., Armstrong, R. N., and Gilliland, G. L. (1993) *Biochemistry 32*, 12949−12954.
59. Oakley, A. J., Lo Bello, M., Mazzetti, A. P., Federici, G., and Parker, M. W. (1997) *FEBS Lett. 419*, 32−36.
60. Ricci, G., Del Boccio, G., Pennelli, A., Lo Bello, M., Petruzzelli, R., Caccuri, A. M., Barra, D., and Federici, G. (1991) *J. Biol. Chem. 266*, 21409−21415.
61. Oakley, A. J., Lo Bello, M., Ricci, G., Federici, G., and Parker, M. W. (1998) *Biochemistry 37*, 9912−9917.
62. Stella, L., Nicotra, M., Ricci, G., Rosato, N., and Di Iorio, E. E. (1999) *Proteins 37*, 1−9.
63. Stella, L., Di Iorio, E. E., Nicotra, M., and Ricci, G. (1999) *Proteins 37*, 10−19.

BI0007122